

DMD 2006/11387

## **Epirubicin Glucuronidation and UGT2B7 Developmental Expression**

Matthew J. Zaya, Ronald N. Hines, and Jeffrey C. Stevens

*Pfizer, 7000 Portage Rd., Kalamazoo, Michigan (M.J.Z.); 800 N. Lindbergh Blvd, St Louis, Missouri (J.C.S.); and The Department of Pediatrics, Medical College of Wisconsin and Children's Research Institute, Children's Hospital and Health System, Milwaukee, Wisconsin (R.N.H.)*

DMD 2006/11387

**Running Title:** Epirubicin glucuronidation and developmental expression

**Corresponding Author:** Matthew J. Zaya

Pfizer, Inc.

7000 Portage Rd.

Kalamazoo, MI 49001

Tel: (269) 833-1189

Fax: (269) 833-7721

E-mail: matthew.j.zaya@pfizer.com

**Number of Text Pages:** 20

**Number of Tables:** 3

**Number of Figures:** 6

**Number of References:** 28

**Abstract Word Length:** 250

**Introduction Word Length:** 436

**Discussion Word Length:** 684

**Abbreviations:** IQR, interquartile range; NFDM, non-fat dry milk; PNA, postnatal age; TBS, Tris Buffered Saline; UDPGA, Uridine diphosphate glucuronic acid; UGT, UDP glucuronosyl transferase

### Abstract

The usefulness of epirubicin in the treatment of adult and childhood malignant diseases is related in part to the potential reduction in cardiac toxicity as compared to other anthracyclines given at equivalent doses. An important pathway for epirubicin detoxification is UGT2B7-dependent glucuronidation. This study was implemented to provide a preclinical evaluation of the metabolism of epirubicin with respect to age-related changes in epirubicin glucuronidation in pediatric liver microsomes. Rates of epirubicin glucuronidation and levels of UGT2B7 were determined for liver microsomes from four pediatric ( $n = 32$ ) and one adult age categories ( $n = 8$ ). Both sets of data showed an increase in UGT2B7 activity and content with increasing age. Epirubicin glucuronidation activity in the adult group was statistically higher compared with all pediatric age groups ( $p \leq 0.01$ ). UGT2B7 expression also was statistically higher in adults compared with children below 11 yrs of age, with evidence of significant differences in protein levels among the pediatric age categories. A positive correlation ( $r = 0.68$ ) between UGT2B7 levels and postnatal age was observed, suggesting a progressive increase in UGT2B7 protein expression with increasing age. However, allometric scaling using the 3/4 power rule suggested no difference in activity between any of the pediatric age categories and the adult, although only a single neonatal sample was included in the analysis. In summary, these in vitro data show differences in epirubicin glucuronidation and UGT2B7 content within pediatric age groups and support the use of epirubicin in pediatric patients at least 6 mos of age.

The anthracycline class of compounds has been used extensively as effective chemotherapeutic agents for a variety of hematological and solid tumors. Anthracyclines are known to be successful in the treatment of childhood related malignancies, with doxorubicin used most frequently (Katzenstein et al. 2003; Kremer et al. 2002). However, the potential myocardial toxicity associated with the cumulative dose of this drug is a major limitation for safe and effective pediatric use. Epirubicin or 4'-epi-doxorubicin, a synthetic derivative of daunorubicin, is a cell cycle phase, non-specific anthracycline and has been utilized as a major component of cancer chemotherapy for a wide spectrum of metastatic diseases, including breast and bladder cancer (Harris et al. 2003; Lunardi et al. 2002; Ormrod et al. 1999). The precise mechanism underlying epirubicin cytotoxicity has not been completely elucidated and safety and efficacy have not been determined in pediatric patients.

Epirubicin and doxorubicin are structurally highly similar, differing only in the orientation of the 4'-hydroxy group. However, this minor difference leads to significant differences in the pharmacokinetics and metabolism of these drugs. Epirubicin is extensively metabolized by the liver to epirubicin glucuronide (Fig. 1) and epirubicinol, with subsequent biliary excretion of the glucuronide conjugate (approx. 25% of dose) (Weenen et al. 1983; Weenen et al. 1984). Using adult human liver microsomes and heterologous enzyme expression systems, this route of epirubicin inactivation was shown to be catalyzed by UDP-glucuronosyltransferase 2B7 (UGT2B7) by Innocenti et al. (2001). Doxorubicin does not share this important detoxification pathway, thus suggesting that epirubicin represents an effective anthracycline possessing a favorable pharmacokinetic profile and fewer toxicological effects (Launchbury et al. 1993; Robert 1993). Clinical pharmacokinetic studies have demonstrated an

DMD 2006/11387

up to 10-fold interpatient variability in epirubicin glucuronidation linked with metabolic clearance, and in vitro metabolism studies have provided evidence that inter-individual variability in rates of glucuronidation appears related to variability in UGT2B7 protein levels. For example, the pharmacokinetics of morphine glucuronidation suggest both age-dependent differences in UGT2B7 activity and significant increases in enzyme expression and/or activity at birth. Adjusting for liver size relative to body weight, adult levels of UGT2B7 are reached by 2-6 mos of age [reviewed in (de Wildt et al. 1999)]. Thus, the developmental pattern for this UGT isoform may provide valuable clinical information in the assessment of epirubicin pediatric pharmacology.

The objective of this study was to conduct a preclinical evaluation of the effect of age on UGT2B7-dependent epirubicin glucuronidation to support a clinical efficacy study in pediatric patients. Using a unique set of pediatric hepatic microsome samples and defined age categories, rates of epirubicin glucuronidation and immunodetectable levels of UGT2B7 were measured and each analyzed for age-dependent change.

## Materials and Methods

**Chemical and Reagents.** Primary antisera containing an antipeptide antibody against UGT2B7 and horseradish peroxidase conjugated goat anti-rabbit antibody were obtained from BD Biosciences (Bedford, MA). Ten percent polyacrylamide Tris-HCl (1.0 mm Criterion™) resolving gels and PVDF transfer membranes (Immun-Blot™) were obtained from Bio-Rad Laboratories (Hercules, CA). Pre-mixed 10X Tris/Glycine/SDS running buffer, 10X Tris/Glycine transfer buffer, and Tween-20 also were obtained from Bio-Rad Laboratories. Sample buffers and reducing agents (NuPAGE™) were obtained from Invitrogen (Carlsbad, CA). Enhanced chemiluminescence blotting reagents (ECL™) and detection film (Hyperfilm™ ECL™) were obtained from Amersham Pharmacia Biotech (Arlington Heights, IL). Tris-buffered-saline buffer (BupH™ Tris buffered saline) was purchased from Pierce Chemical Company (Rockford, IL). Epirubicin HCl and alamethicin were obtained from Pharmacia (Nerviano, Italy and Kalamazoo, MI, respectively). Daunorubicin,  $\beta$ -glucuronidase, and UDP-glucuronic acid (UDPGA) were obtained from Sigma-Aldrich (St. Louis, MO). All other reagents and materials were obtained from common commercial sources at the highest grade available.

**Microsomes.** Pediatric liver samples were obtained and microsome fractions prepared as described previously (Koukouritaki et al. 2002). The age categories for the donor liver microsome samples are given in Table 1. Pooled human liver microsomes were obtained from Xenotech LLC (Kansas City, KS) and individual adult liver microsomes were obtained from the

DMD 2006/11387

Pfizer/Pharmacia liver microsome bank. Microsomes from insect cells infected with baculovirus expressing recombinant UGT2B7 were obtained from BD Biosciences (Bedford, MA).

**Epirubicin Glucuronidation Assay.** Kinetic reactions with expressed UGT2B7 and pooled human liver microsomes were performed using a 100  $\mu$ l reaction mixture containing 0.5 mg/ml microsomal protein, 5.0 mM UDPGA, and 25-1200  $\mu$ M epirubicin in 50 mM Tris-HCl/8 mM MgCl<sub>2</sub> (pH 7.5) buffer containing alamethicin (50  $\mu$ g/mg protein) and incubated in a shaking water bath at 37°C for 15 min. Reactions with pediatric and adult liver microsomes were performed using 500  $\mu$ M epirubicin, 0.2 mg/ml protein and 30 min incubation times under the same conditions described above. Chilled samples were pre-incubated at 37°C for 3 minutes and all reactions were initiated with the addition of 5 mM UDPGA to the reaction mixture. The reaction was terminated by the addition of 25  $\mu$ l cold acetonitrile/0.03% phosphoric acid containing 100  $\mu$ M daunorubicin as the internal standard and centrifuged at 10,000 x g for 3 minutes. A 50  $\mu$ l aliquot of the supernatant was used for HPLC analysis. Preliminary experiments showed the glucuronidation assay was linear under conditions of a 30 minute incubation and 0.5 mg microsomal protein.

Epirubicin, epirubicin glucuronide and daunorubicin were detected using a Perkin Elmer Series 200 HPLC system (Perkin Elmer, San Jose, CA) with fluorescence detection at 480 ( $\lambda_{ex}$ ) and 560 ( $\lambda_{em}$ ) nm using a Waters™ 474 fluorescence scanning detector (Water Corp., Milford, MA). Separation was accomplished at room temperature using a reversed phase Supelcosil™ LC-CN column (4.6 x 250 mm, 5  $\mu$ m, Supelco Inc., Bellefonte, PA) preceded by a SecurityGuard™ phenyl guard cartridge (Phenomenex, Torrance, CA) and a mobile phase consisting of 30% acetonitrile and 70% 50 mM sodium dihydrogen phosphate (pH 4.0) at a flow

DMD 2006/11387

rate of 0.8 ml/min. The quantitation of the epirubicin glucuronide metabolite was performed by comparing chromatographic peak heights to a standard curve of 0.5 to 5.0 nmol epirubicin/ml constructed due to the unavailability of pure epirubicin glucuronide. The assumption that the fluorescence of epirubicin glucuronide was equal to that of epirubicin is based on the comparative fluorescence spectra and has been utilized in related studies (Barker et al. 1996). Identification of the epirubicin glucuronide chromatographic peak by enzymatic hydrolysis with  $\beta$ -glucuronidase was performed by treatment of a human liver microsome incubation sample with 1000 IU of  $\beta$ -glucuronidase (type VII, from *Escherichia coli*) in 0.1 M sodium phosphate buffer, pH 6.8 at 37°C overnight and analyzed as described above.

**Electrophoresis and immunoblotting.** Proteins were separated by sodium dodecyl sulfate-polyacrylamide gel electrophoresis (SDS-PAGE) using 10% acrylamide resolving gels and a Tris-glycine running buffer (Laemmli1970). A 2-3  $\mu$ g aliquot of microsomal protein from each sample was analyzed. Separation was carried out using the Criterion™ Precast Gel Electrophoresis System (Bio-Rad Laboratories) and proteins were transferred to polyvinylidene difluoride membranes using the Criterion™ blotter according to the manufacturer's instructions. Membranes were blocked with 5% nonfat dry milk (NFDM) in Tris-buffered saline (TBS; 25 mM Tris, 150 mM sodium chloride, pH 7.5). The transfer membranes were incubated for 1 h at room temperature with UGT2B7 primary antibody diluted 1:500 in TBS containing 1% NFDM and 0.05% Tween-20. The membranes were then washed several times with TBS containing 0.1% Tween-20 and incubated for 1 h at room temperature with the HRP-labeled secondary antibody diluted 1:500 in TBS containing 1% NFDM and 0.05% Tween-20. Membranes were then washed several times with TBS containing 0.1% Tween-20 and processed for UGT2B7



DMD 2006/11387

detection by enhanced chemiluminescence according to the manufacturer's instructions. The luminescence produced was detected by exposure to film and scanned using a Bio-Rad GS-710 calibrated imaging densitometer. Using a standard curve representing 0.01 to 0.25  $\mu\text{g}$  expressed human UGT2B7 distributed on each membrane, immunoreactive protein bands were quantified using linear regression (Quantity One™ software, Bio-Rad Laboratories).

**Statistical Analysis.** Data from rates of epirubicin glucuronidation and UGT2B7 protein levels were analyzed with the statistical analysis package Unistat (Unistat V5.0, London UK). These data were analyzed by the Kruskal-Wallis non-parametric analysis of variance (ANOVA) (Hollander et al. 1999). Multiple comparisons were made using the t distribution on the mean ranks. Correlation analysis was performed using GraphPad Prism V3.0 (San Diego CA). Epirubicin glucuronidation activities that were normalized by scaling to a 70 kg individual using the 3/4 power rule (Holford 1996) were compared using one-way ANOVA (SigmaStat V 3.11, SysStat Software, Point Richmond, CA). An  $\alpha$  value of  $p < 0.05$  was accepted as significant.

## Results

**Kinetic analysis of epirubicin glucuronidation.** A description of incubation conditions and kinetic parameters for epirubicin glucuronidation has been reported (Innocenti et al. 2001); however, the limiting quantities of each sample for the current study necessitated incubations using substantially reduced concentrations of microsomal protein. Briefly, under conditions of saturating substrate, less than 4% of the parent compound was consumed using lower protein concentrations (incubations of human liver microsome samples at 0.2 mg protein/ml or 20  $\mu$ g total protein and expressed UGT2B7 at 0.5 mg/ml or 50  $\mu$ g total protein) for the respective incubation durations. Kinetic evaluations of epirubicin glucuronidation were performed using the above conditions with increasing concentrations of substrate. The resulting activities were fit to a single enzyme model ( $r^2 = 0.9936$ ) (data not shown). For a pooled adult human liver microsome sample, apparent  $K_m$  ( $K_{m,app}$ ) and maximal reaction rate ( $V_{max}$ ) were 213  $\mu$ M and 3.56 nmol epirubicin glucuronide formed/min/mg protein. For expressed UGT2B7, the calculated  $K_m$  was 46  $\mu$ M with a  $V_{max}$  of 0.86 nmol/min/mg protein.

**Age-dependent differences in epirubicin glucuronidation.** The rate of epirubicin glucuronidation was evaluated for 4 pediatric categories and 1 adult age category, each consisting of eight samples. Due to the limited number of available samples, categories were determined *a priori* to include this balanced observation approach rather than by regression tree analysis and node identification. Fig. 2 shows the box and whisker plot for epirubicin glucuronidation by age category. The statistical analysis showed no strong difference between mean rank values among the four pediatric age categories ( $p > 0.05$ , Table 2) except the 12-17 yr

DMD 2006/11387

age category, which was different from the <1 yr category ( $p = 0.02$ ). Rates of epirubicin glucuronidation for pediatric samples showed high intersubject variability, particularly within the 6-11 yr and 12-17 yr categories. The adult category was characterized by lower interindividual variability (3-fold) and a high average activity (2.1 nmol/min/mg) that was statistically different from each of the pediatric categories ( $p \leq 0.05$ ).

**Immunoquantitation of UGT2B7 protein.** Since previous studies have identified UGT2B7 as the primary catalyst of epirubicin glucuronidation, the ontogeny of UGT2B7 expression was investigated. Fig. 3 shows that a 25-fold dynamic range of UGT2B7 immunoquantitation could be obtained using the expressed enzyme, as detection of the 0.005  $\mu$ g sample was not reliable (lanes 1-6). An immunoreactive protein of similar molecular weight to expressed UGT2B7 was observed for six of eight samples from the <1 yr pediatric category (lanes 8-15) and from all other human liver microsome samples analyzed (data not shown). Fig. 4 shows the box and whisker plots for human liver microsome UGT2B7 protein levels by age category. The results follow a pattern similar to that observed for rates of epirubicin glucuronidation by age category in that a statistical difference was observed between the adult group when compared to each of the pediatric groups except 12-17 yrs. The latter approached significance ( $p = 0.057$ ). Average levels of UGT2B7 protein showed an age-dependent increase and the differences in the pediatric age groups were significant for the 12-17 yr age group when compared with the <1 and 1-5 yr age groups ( $p < 0.001$ ). The 6-11 yr age group also showed a statistical difference compared to the <1 yr age ( $p < 0.001$ ) and the 1-5 yr group ( $p = 0.0086$ ).

**Correlation analysis.** A useful approach for reaction phenotype analysis of cytochrome P450- dependent processes is the correlation of marker enzyme activities with immunodetectable

DMD 2006/11387

protein levels within a defined set of liver microsome samples (Parkinson 1996). Therefore, this approach was applied to compare UGT2B7 protein levels with rates of epirubicin glucuronidation for all human liver microsome samples analyzed (Fig. 5). These two parameters were significantly correlated ( $r = 0.86$ ,  $p < 0.001$ ), thus further implicating UGT2B7 as the primary catalyst in epirubicin glucuronidation. Each of these parameters was then independently analyzed versus the postnatal age of the human liver sample donor. Fig. 6A shows the rates of epirubicin glucuronidation with increasing postnatal age for the pediatric liver microsome samples. These variables showed a weak but significant correlation ( $r = 0.36$ ,  $p < 0.05$ ). A similar analysis of liver microsomal UGT2B7 levels versus postnatal age showed a stronger correlation ( $r = 0.68$ ,  $p < 0.001$ ) (Fig. 6B). Together these results suggest an age-dependent increase for UGT2B7-dependent epirubicin glucuronidation that was not discernable from the predefined age categories (Figs. 2 and 4).

## Discussion

The use of the anthracycline, doxorubicin, as a chemotherapeutic agent in children has generated considerable concern regarding long-term safety. The development of the less toxic anthracycline derivative, epirubicin, has resulted in a more widespread use of this class of agents for childhood cancer. However, a careful comparison between doxorubicin and epirubicin pharmacokinetics and pharmacodynamics suggests the decreased toxicity of the latter is due to its metabolism and clearance by UGT2B7. Thus, an assessment of the postnatal developmental expression pattern of human hepatic UGT2B7 and more specifically, the possible changes in activity toward epirubicin, were considered important in the assessment of age-dependent pharmacokinetic changes and variability of this drug in the pediatric population.

The kinetic constants determined in the current study ( $K_{m,app} = 213 \mu\text{M}$  and  $V_{max} = 3.56 \text{ nmol/min/mg}$  for pooled microsomes;  $K_m = 46 \mu\text{M}$  and  $V_{max} = 0.86 \text{ nmol/min/mg}$  for expressed recombinant protein) are different from those previously reported ( $K_m$  values of  $568 \mu\text{M}$  and  $149 \mu\text{M}$  for human liver microsomes and expressed UGT2B7, respectively). These comparatively higher affinity constants may be attributable to the higher microsomal protein concentration used by these investigators ( $3 \text{ mg/ml}$  microsomal protein). Although not measured experimentally in the current study, non-specific microsomal protein binding is well documented for producing increased relative affinity parameters for in vitro studies (Kalvass et al. 2001; Obach 1999). The 4-fold difference in apparent  $K_m$  values between human liver microsomes and the expressed microsomal UGT2B7 enzyme has been previously noted and may be attributable to, a) the involvement of an unidentified higher affinity human liver UGT form in the glucuronidation of

epirubicin, b) the influence of incubation conditions or the lipid environment of the microsomal preparations (Fisher et al. 2000; Rimmel et al. 1993; Soars et al. 2003), or c) alteration of UGT kinetics and activity due to oligimerization (Ikushiro et al. 1997; Ishii et al. 2001; Meech et al. 1997).

An examination of epirubicin glucuronidation activity in pediatric liver microsomes demonstrated a median activity in tissue from individuals less than one yr of age that was approximately 10% of that observed in tissue from adults. Between one yr of age and puberty (11 yrs of age), median enzyme activity was 25% of that seen in adults whereas between 12 and 17 yrs of age, the observed median activity was approximately 50% of the observed adult value. These relative values are corroborated by the immunological determination of UGT2B7 content, which correlated well with enzyme activity ( $r = 0.86$ ). However, if one normalizes the pediatric data to a 70 kg individual using the 3/4 power rule, no significant differences are observed among the different developmental age groups or between any of the pediatric age groups and adults (Table 3) ( $p = 0.138$ ). These data are consistent with morphine clearance in pediatric patients by glucuronidation, a well-documented marker of UGT2B7 activity (Coffman et al. 1997). Morphine clearance was 5-fold higher in children 1 to 16 yrs of age versus neonates, but clearance values matching adults were attained between 6 and 30 mos when calculated using a per-kg size model (Choonara et al. 1989). When scaled using the 3/4 power model, adult levels of morphine clearance were attained between 2 and 6 mos of age (Anderson et al. 1997). In the current data set, only one of the tissue samples analyzed was from a neonate, only two were from individuals less than 2 mos of age and the median age of all samples less than one yr of age was 4.8 mos.

DMD 2006/11387

In summary, epirubicin glucuronidation activity and content clearly vary directly as a function of increasing age. However, when pediatric data was normalized using  $3/4$  power allometric scaling, epirubicin glucuronidation activity in all pediatric age categories was not found to be statistically different from activities determined for the adult liver samples. These data are consistent with data on the ontogeny of morphine glucuronidation wherein adult activity values are attained by 2 to 6 mos of age. Thus, the data presented in the current study would support the use of epirubicin as a cancer chemotherapeutic agent in pediatric patients older than 6 mos of age.

## References

- Anderson BJ, McKee AD, and Holford NH (1997) Size, myths and the clinical pharmacokinetics of analgesia in paediatric patients. *Clin Pharmacokinet* 33:313-327.
- Barker IK, Crawford SM, and Fell AF (1996) Determination of plasma concentrations of epirubicin and its metabolites by high-performance liquid chromatography during a 96-h infusion in cancer chemotherapy. *J Chromatogr B Biomed Appl* 681:323-329.
- Choonara IA, McKay P, Hain R, and Rane A (1989) Morphine metabolism in children. *Br J Clin Pharmacol* 28:599-604.
- Coffman BL, Rios GR, King CD, and Tephly TR (1997) Human UGT2B7 catalyzes morphine glucuronidation. *Drug Metab Dispos* 25:1-4.
- de Wildt SN, Kearns GL, Leeder JS, and van den Anker JN (1999) Glucuronidation in humans: Pharmacogenetic and developmental aspects. *Clin Pharmacokinet* 36:439-452.
- Fisher MB, Campanale K, Ackermann BL, Vandenbranden M, and Wrighton SA (2000) In vitro glucuronidation using human liver microsomes and the pore-forming peptide alamethicin. *Drug Metab Dispos* 28:560-566.
- Harris NM, Anderson WR, Lwaleed BA, Cooper AJ, Birch BR, and Solomon LZ (2003) Epirubicin and meglumine gamma-linolenic acid: a logical choice of combination therapy for patients with superficial bladder carcinoma. *Cancer* 97:71-78.
- Holford NH (1996) A size standard for pharmacokinetics. *Clin Pharmacokinet* 30:329-332.
- Hollander M and Wolfe DA (1999) *Nonparametric statistical methods*. John Wiley and Sons, New York.



- Ikushiro S, Emi Y, and Iyanagi T (1997) Protein-protein interactions between UDP-glucuronosyltransferase isozymes in rat hepatic microsomes. *Biochemistry* 36:7154-7161.
- Innocenti F, Iyer L, Ramirez J, Green MD, and Ratain MJ (2001) Epirubicin glucuronidation is catalyzed by human UDP-glucuronosyltransferase 2B7. *Drug Metab Dispos* 29:686-692.
- Ishii Y, Miyoshi A, Watanabe R, Tsuruda K, Tsuda M, Yamaguchi-Nagamatsu Y, Yoshisue K, Tanaka M, Maji D, Ohgiya S, and Oguri K (2001) Simultaneous expression of guinea pig UDP-glucuronosyltransferase 2B21 and 2B22 in COS-7 cells enhances UDP-glucuronosyltransferase 2B21-catalyzed morphine-6-glucuronide formation. *Mol Pharmacol* 60:1040-1048.
- Kalvass JC, Tess DA, Giragossian C, Linhares MC, and Maurer TS (2001) Influence of microsomal concentration on apparent intrinsic clearance: implications for scaling in vitro data. *Drug Metab Dispos* 29:1332-1336.
- Katzenstein HM, Krailo MD, Malogolowkin MH, Ortega JA, Qu W, Douglass EC, Feusner JH, Reynolds M, Quinn JJ, Newman K, Finegold MJ, Haas JE, Sensel MG, Castleberry RP, and Bowman LC (2003) Fibrolamellar hepatocellular carcinoma in children and adolescents. *Cancer* 97:2006-2012.
- Koukouritaki SB, Simpson P, Yeung CK, Rettie AE, and Hines RN (2002) Human hepatic flavin-containing monooxygenase 1 (*FMO1*) and 3 (*FMO3*) developmental expression. *Pediatric Res* 51:236-243.
- Kremer LC, van der Pal HJ, Offringa M, van Dalen EC, and Voute PA (2002) Frequency and risk factors of subclinical cardiotoxicity after anthracycline therapy in children: a systematic review. *Ann Oncol* 13:819-829.

- Laemmli UK (1970) Cleavage of structural proteins during the assembly of the head of the bacteriophage T4. *Nature* 227:680-685.
- Launchbury AP and Habboubi N (1993) Epirubicin and doxorubicin: a comparison of their characteristics, therapeutic activity and toxicity. *Cancer Treat Rev* 19:197-228.
- Lunardi G, Venturini M, Vannozzi MO, Tolino G, Del ML, Bighin C, Schettini G, and Esposito M (2002) Influence of alternate sequences of epirubicin and docetaxel on the pharmacokinetic behaviour of both drugs in advanced breast cancer. *Ann Oncol* 13:280-285.
- Meech R and Mackenzie PI (1997) UDP-glucuronosyltransferase, the role of the amino terminus in dimerization. *J Biol Chem* 272:26913-26917.
- Obach RS (1999) Prediction of human clearance of twenty-nine drugs from hepatic microsomal intrinsic clearance data: An examination of in vitro half-life approach and nonspecific binding to microsomes. *Drug Metab Dispos* 27:1350-1359.
- Ormrod D, Holm K, Goa K, and Spencer C (1999) Epirubicin: a review of its efficacy as adjuvant therapy and in the treatment of metastatic disease in breast cancer. *Drugs Aging* 15:389-416.
- Parkinson A (1996) An overview of current cytochrome P450 technology for assessing the safety and efficacy of new materials. *Toxicol Path* 24:48-57.
- Rommel RP and Burchell B (1993) Validation and use of cloned, expressed human drug-metabolizing enzymes in heterologous cells for analysis of drug metabolism and drug-drug interactions. *Biochem Pharmacol* 46:559-566.
- Robert J (1993) Epirubicin. Clinical pharmacology and dose-effect relationship. *Drugs* 45 Suppl 2:20-30.

DMD 2006/11387

Soars MG, Ring BJ, and Wrighton SA (2003) The effect of incubation conditions on the enzyme kinetics of udp-glucuronosyltransferases. *Drug Metab Dispos* 31:762-767.

Weenen H, Lankelma J, Penders PG, McVie JG, ten Bokkel Huinink WW, de Planque MM, and Pinedo HM (1983) Pharmacokinetics of 4'-epi-doxorubicin in man. *Invest New Drugs* 1:59-64.

Weenen H, van Maanen JM, de Planque MM, McVie JG, and Pinedo HM (1984) Metabolism of 4'-modified analogs of doxorubicin. unique glucuronidation pathway for 4'-epidoxorubicin. *Eur J Cancer Clin Oncol* 20:919-926.

### Legends for Figures

Fig. 1. *Structural formula of epirubicin and epirubicin glucuronide.*

Fig. 2. *Box and whisker plot analysis of in vitro epirubicin glucuronidation activity as a function of age.* Activity levels (pmol epirubicin glucuronide formed/min/mg microsomal protein) were quantitated as described in Materials and Methods. The bottom and top of the boxes represent the 25<sup>th</sup> and 75<sup>th</sup> percentiles respectively. The solid horizontal line within each box represents the median value. The horizontal dash within each box represents the mean value. The lower whisker is equal to the maximum of (i) lower quartile minus 1.5 times the inter-quartile range (IQR) and (ii) the minimum observation within the IQR. The upper whisker is equal to the minimum of (i) the 75<sup>th</sup> percentile plus 1.5 times the IQR and (ii) the maximum observation within the IQR.

Fig. 3. *Immunoblot analysis of UGT2B7 protein in human liver microsomes.* Lanes 1-6 contain 0.005, 0.01, 0.025, 0.050, 0.10 and 0.25  $\mu$ g expressed UGT2B7, respectively. Lane 7 contains UGT insect control microsomal protein and lanes 8-15 include samples from the <1 yr postnatal age group (3  $\mu$ g of total protein per analysis). Lane 16 contains pooled human liver microsomes (3  $\mu$ g). Electrophoresis and immunodetection using an antibody to UGT2B7 were conducted as described in Materials and Methods.

DMD 2006/11387

Fig. 4. *Box and whisker plot analysis of immunodetectable UGT2B7 determined for pediatric and adult liver microsomal samples.* Protein levels ( $\mu\text{g}$  expressed UGT2B7/mg microsomal protein) were quantitated as described in Materials and Methods. The bottom and top of the boxes represent the 25<sup>th</sup> and 75<sup>th</sup> percentiles respectively. The solid horizontal line within each box represents the median value. The horizontal dash within each box represents the mean value. The lower whisker is equal to the maximum of (i) lower quartile minus 1.5 times the inter-quartile range (IQR) and (ii) the minimum observation within the IQR. The upper whisker is equal to the minimum of (i) the 75<sup>th</sup> percentile plus 1.5 times the IQR and (ii) the maximum observation within the IQR.

Fig. 5. *Correlation between epirubicin glucuronidation and UGT2B7 protein content in adult and pediatric liver microsomes.* The correlation coefficient ( $r = 0.86$ ) was statistically significant ( $p < 0.0001$ ); ( $r^2 = 0.74$ ,  $n = 40$ ).

Fig. 6. *Correlation between (i) epirubicin glucuronidation activity and UGT2B7 content and postnatal age.* (A) Correlation between epirubicin glucuronidation activity and postnatal age (PNA) in pediatric liver microsomes ( $n = 32$ ). Coefficient of determination ( $r^2$ ) = 0.13. The correlation coefficient ( $r = 0.36$ ,  $p = 0.047$ ). (B) Correlation between UGT2B7 content and postnatal age (PNA) in pediatric liver microsomes ( $n = 32$ ). Coefficient of determination ( $r^2$ ) = 0.47. The correlation coefficient ( $r = 0.68$ ,  $p < 0.0001$ ).

## Tables

TABLE 1. *Age category definitions for pediatric and adult liver microsome samples.*

The age range categories included eight individual samples each. Samples were selected so that the entire range of the category was represented. A total of 40 individual samples were analyzed for UGT activity and immunodetectable UGT2B7 levels.

<b>Age Range (PNA)<sup>a</sup></b>	<b>Age Category</b>
0 - 316	<1 yr
415 - 1825	1 - 5 yrs
2208 - 4015	6 - 11 yrs
4534 - 6233	12 - 17 yrs
>6570	>18 yrs - adult

<sup>a</sup> PNA: postnatal age in days

TABLE 2. *Statistical analysis of category comparisons for rates of epirubicin glucuronidation and levels of liver microsomal UGT2B7 protein.*

Statistical methods are described in Materials and Methods.

<b>Rate of Glucuronidation</b>		<b>Immunodetectable UGT2B7</b>	
<b>Age Category</b>	<b>P Value</b>	<b>Age Category</b>	<b>P Value</b>
<1 vs 1 - 5	0.5274	<1 vs 1 - 5	0.2054
<1 vs 6 - 11	0.0674	<1 vs 6 - 11	0.0003
<1 vs 12 - 17	0.0211	<1 vs 12 - 17	<0.0001
<1 vs Adult	<0.0001	<1 vs Adult	<0.0001
1 - 5 vs 6 - 11	0.2199	1 - 5 vs 6 - 11	0.0086
1 - 5 vs 12 - 17	0.0844	1 - 5 vs 12 - 17	0.0007
1 - 5 vs Adult	0.0001	1 - 5 vs Adult	<0.0001
6 - 11 vs 12 - 17	0.6013	6 - 11 vs 12 - 17	0.3655
6 - 11 vs Adult	0.0032	6 - 11 vs Adult	0.0066
12 - 17 vs Adult	0.0124	12 - 17 vs Adult	0.0569

TABLE 3. *Scaled UGT2B7 activity as a function of age*

<b>Group</b>	<b>N</b>	<b>Scaled UGT2B7 Activity<sup>a</sup> (pmol/min/mg protein)</b>
Age <1 yr	8	2008.2 ± 1681.3
Age 1 - 5 yrs	7	1648.2 ± 830.2
Age 6 - 11 yrs	6	1096.2 ± 867.3
Age 12 - 17 yrs	7	992.7 ± 680.1
Adult	8	2101.0 ± 743.0

<sup>a</sup> Individual pediatric activities were scaled and normalized to a 70 kg individual using the 3/4 power allometric rule ( $\text{Activity}_{70\text{kg}} = \text{Activity}_i / (\text{Weight}_i / 70 \text{ kg})^{0.75}$ , where  $\text{Activity}_i$  and  $\text{Weight}_i$  are the activity and weight of the individual pediatric samples, respectively). Data are expressed as mean ± SD.



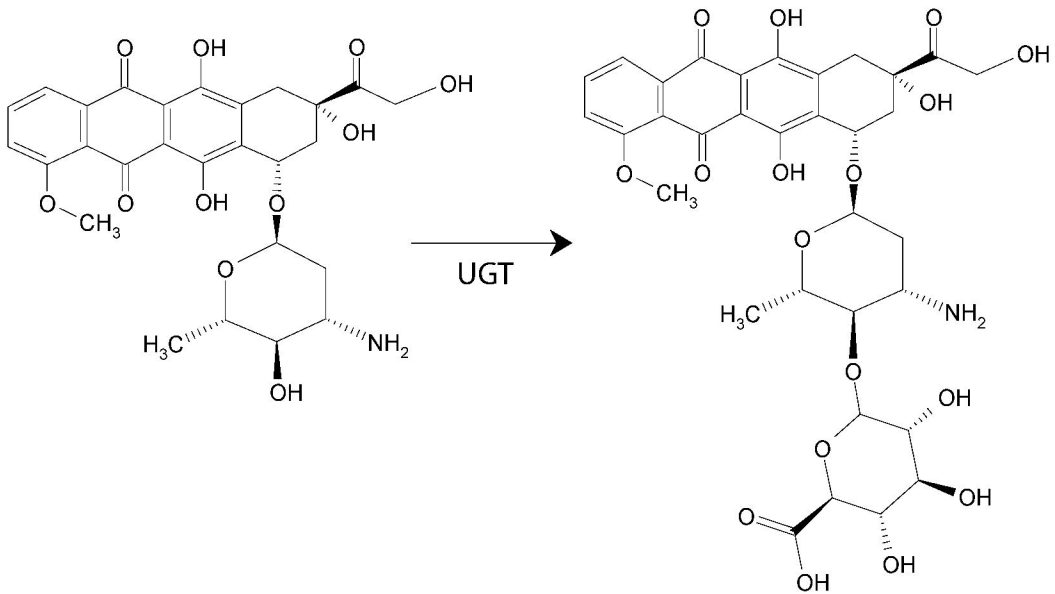


Figure 1

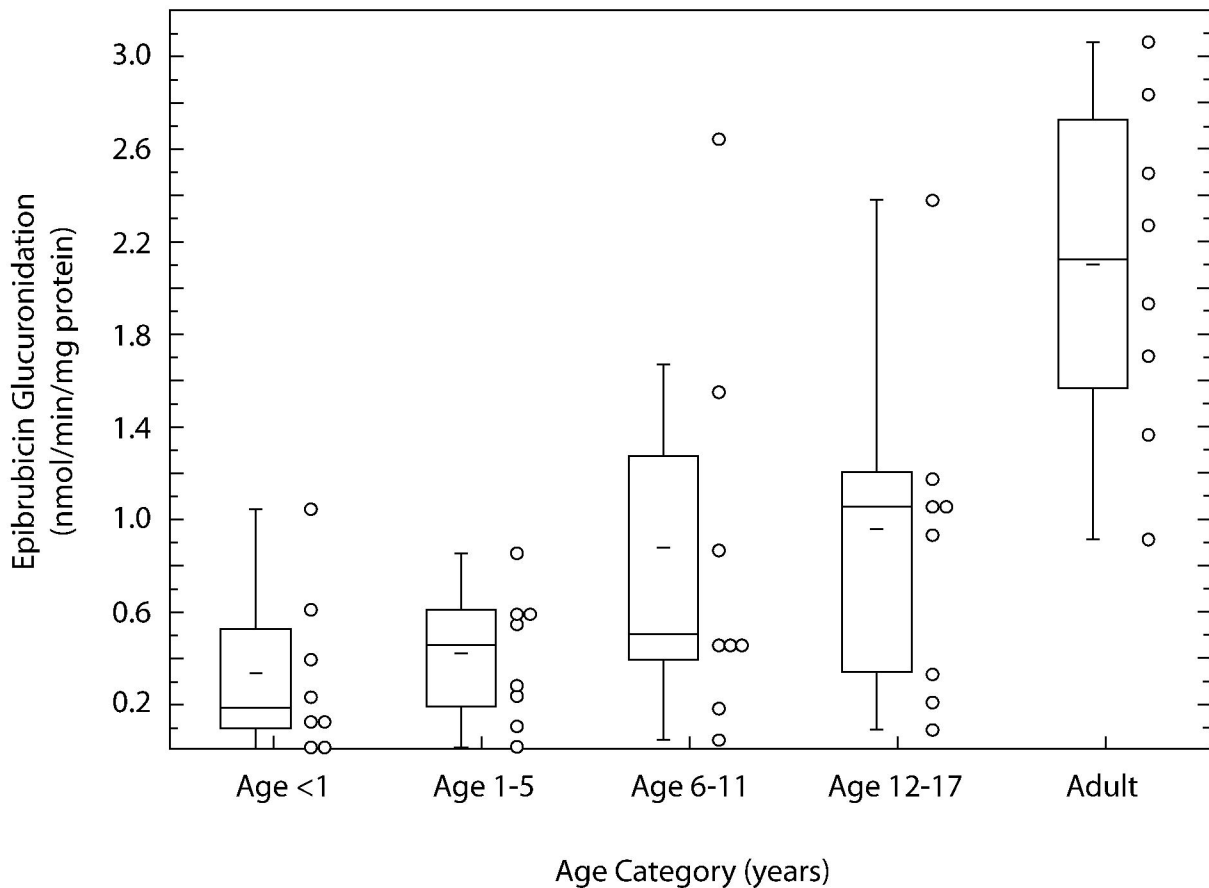


Figure 2



1 2 3 4 5 6 7 8 9 10 11 12 13 14 15 16

Figure 3

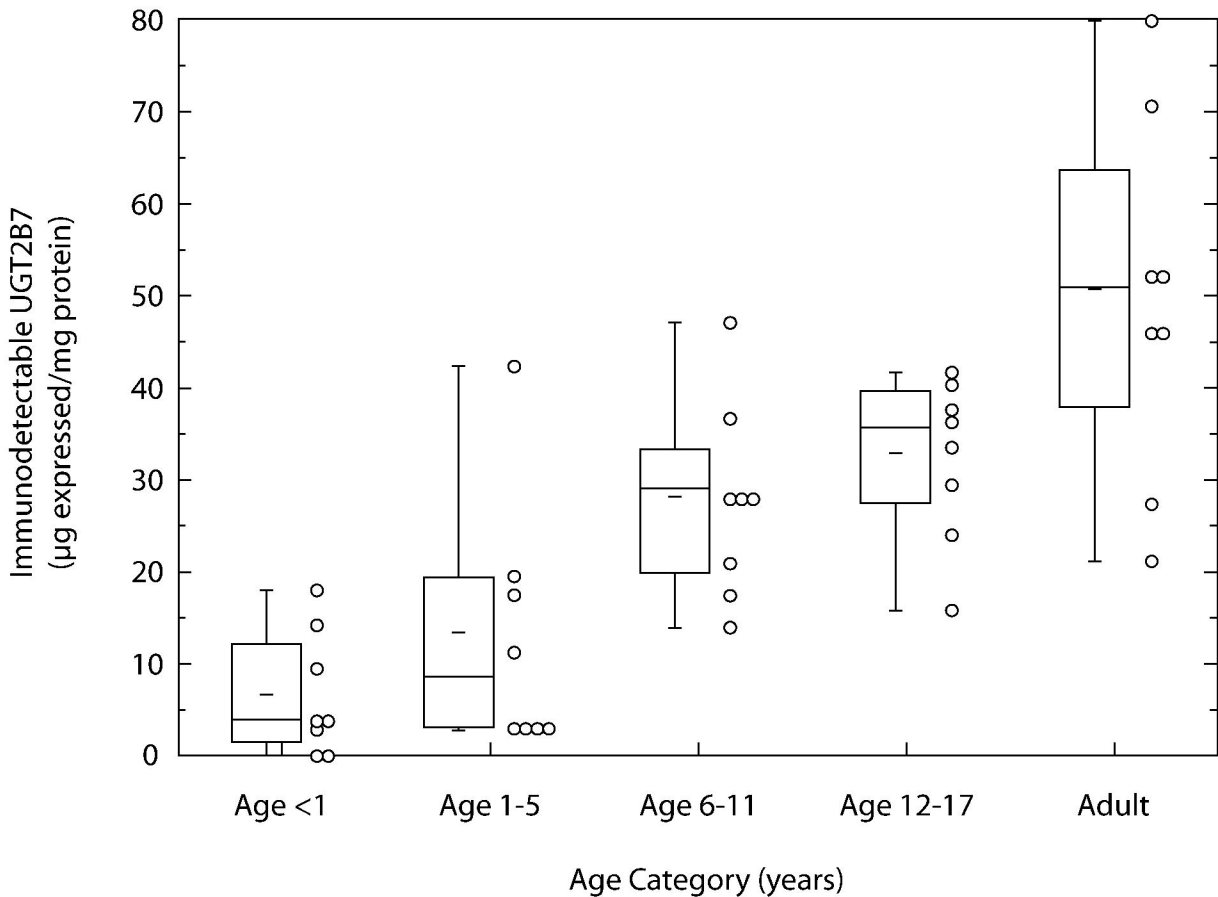


Figure 4

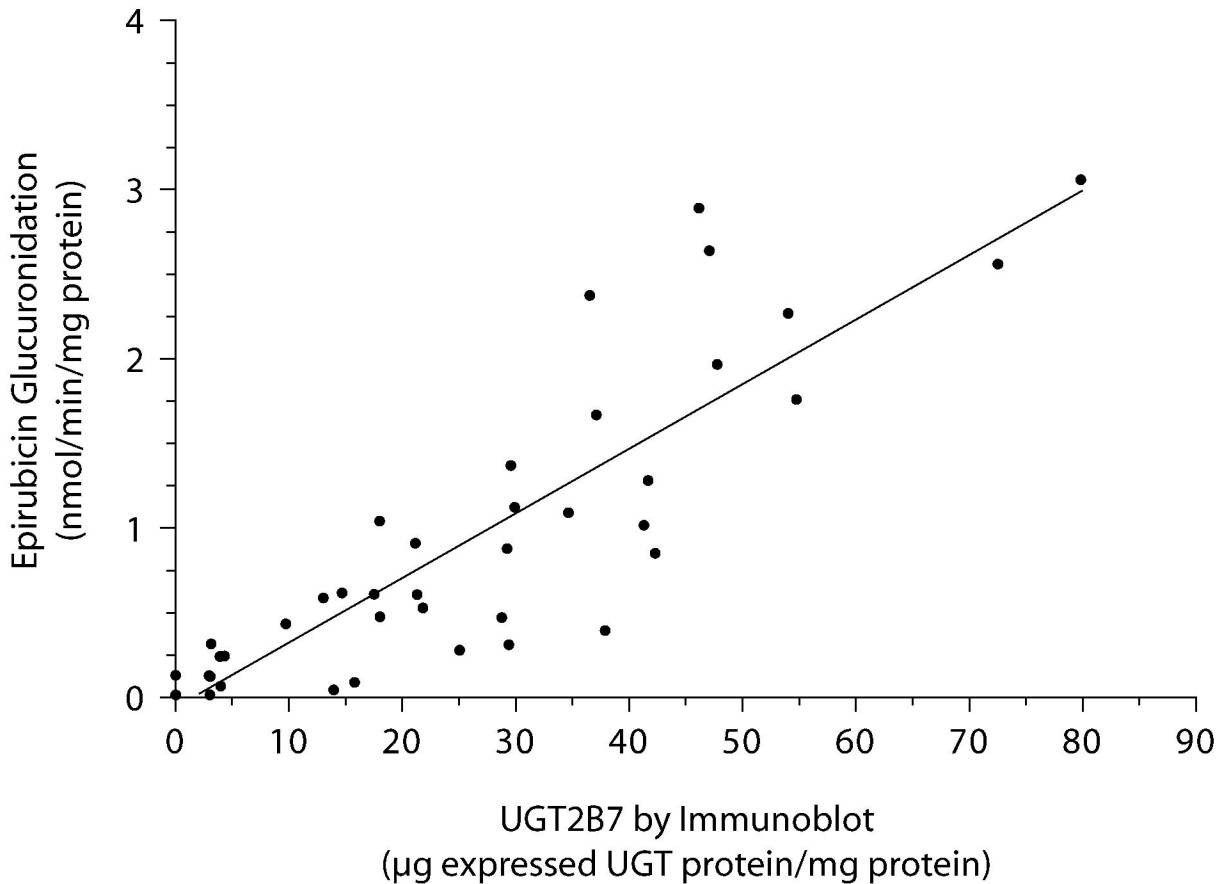


Figure 5

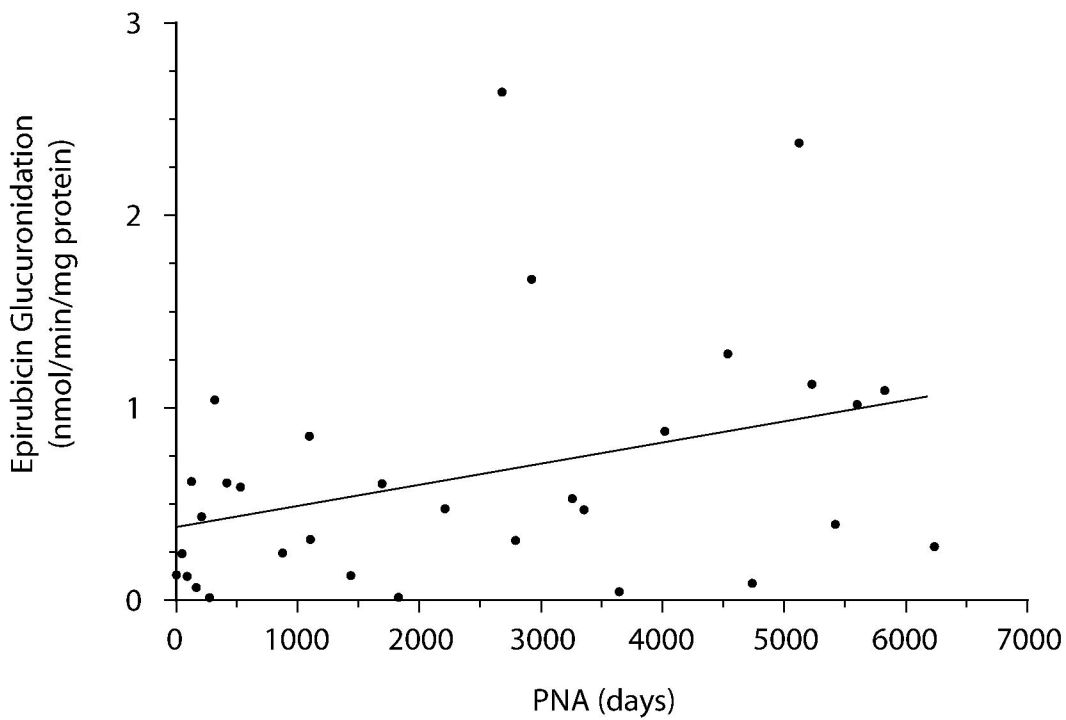
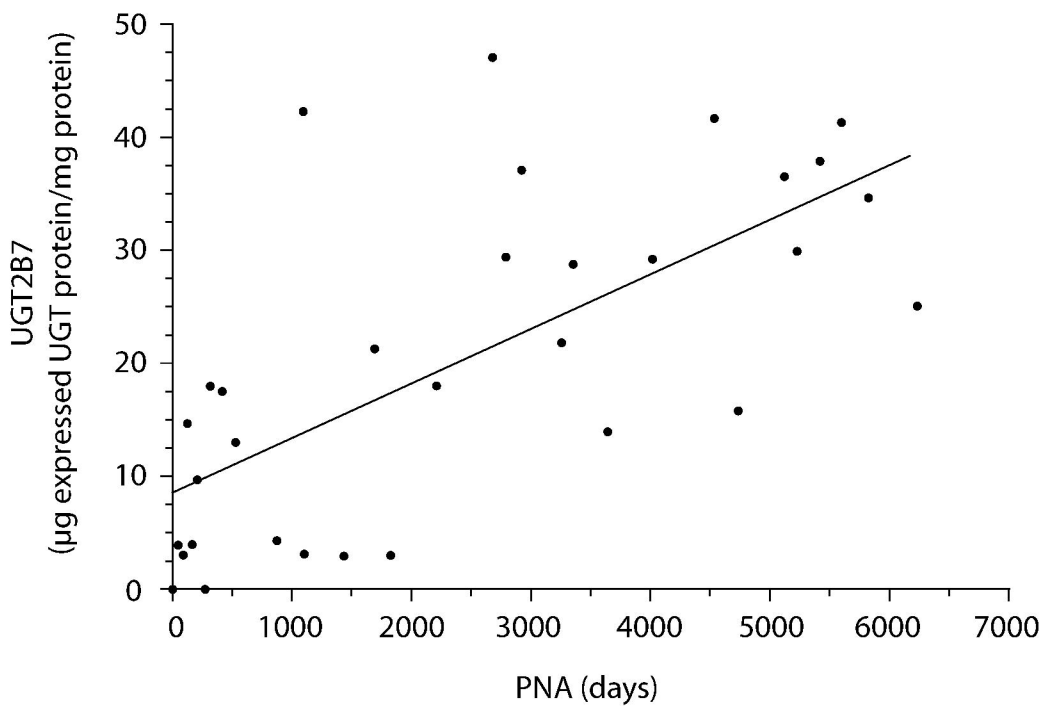
**A****B**

Figure 6